

1
2
3
4
5
6
7
8
9
10
11
12
13
14
15
16
17
18
19
20
21
22
23
24
25
26
27
28
29
30
31
32
33
34
35
36
37
38
39
40
41
42
43
44
45
46

Diverse patterns of ocean export productivity change across the Cretaceous-Paleogene boundary: new insights from biogenic barium

Pincelli M. Hull^{1,2} and Richard D. Norris¹

¹Scripps Institution of Oceanography, University of California San Diego, 9500 Gilman Drive
MC 0244, La Jolla, California, 92093-0244

²Present address: Yale University, Department of Geology and Geophysics, PO Box 208109,
New Haven, Connecticut, 06520-8109

*Corresponding author: pincelli.hull@yale.edu

46 **ABSTRACT**

47 One of the best-studied aspects of the K-Pg mass extinction is the decline and subsequent
48 recovery of open ocean export productivity (e.g., the flux of organic matter from the surface to
49 deep ocean). Some export proxies, including surface-to-deep water $\delta^{13}\text{C}$ gradients and carbonate
50 sedimentation rates, indicate a global decline in export productivity triggered by the extinction.
51 In contrast, benthic foraminiferal and other geochemical productivity proxies suggest spatially
52 and temporally heterogeneous K-Pg boundary effects. Here we address these conflicting export
53 productivity patterns using new and compiled measurements of biogenic barium. Unlike a
54 previous synthesis, we find that the boundary effect on export productivity and the timing of
55 recovery varied considerably between different oceanic sites. The northeast and southwest
56 Atlantic, Southern Ocean and Indian Ocean records saw export production plummet and remain
57 depressed for 350 thousand to 2 million years. Biogenic barium and other proxies in the central
58 Pacific and some upwelling or neritic Atlantic sites indicate the opposite, with proxies recording
59 either no change or increased export production in the early Paleocene. Our results suggest that
60 widespread declines in surface-to-deep ocean $\delta^{13}\text{C}$ do not record a global decrease in export
61 productivity. Rather, independent proxies –including barium and other geochemical proxies, and
62 benthic community structure– indicate that some regions were characterized by maintained or
63 rapidly recovered organic flux from the surface ocean to the deep sea floor, while other regions
64 had profound reductions in export productivity that persisted long into the Paleocene.

65

65 **1. INTRODUCTION**

66 The Cretaceous-Paleogene (K-Pg) mass extinction provides a natural experiment in
67 processes of extinction and recovery, as it is the most recent and well studied of the five major
68 mass extinctions. The K-Pg extinction was triggered by the Chicxulub impact [e.g., *Bralower et*
69 *al.*, 2010; *Miller et al.*, 2010; *Schulte et al.*, 2010] and is thought to have precipitated a sudden
70 decrease in primary and/or export productivity in the global ocean [*Hsü et al.*, 1982b; *Zachos et*
71 *al.*, 1989; *D'Hondt et al.*, 1998]. A decrease in organic matter export from the surface ocean is
72 indicated by the collapse of surface-to-deep water $\delta^{13}\text{C}$ gradients in carbonates, a sharp decrease
73 in biogenic sedimentation rates, and improved carbonate preservation [*Hsü et al.*, 1982a; *Stott*
74 *and Kennett*, 1989; *Zachos et al.*, 1989; *D'Hondt*, 2005]. In the aftermath of the K-Pg extinction,
75 the recovery to pre-impact levels of surface-to-deep $\delta^{13}\text{C}$ gradients coincided with the re-
76 diversification of planktonic foraminiferal species richness [*Coxall et al.*, 2006]. This diversity-
77 $\delta^{13}\text{C}$ correlation is striking, and has been interpreted to suggest that stable, species-rich ocean
78 ecosystems are either necessary for and/or dependent on relatively high export production
79 [*D'Hondt et al.*, 1998; *Coxall et al.*, 2006].

80 There have been two primary hypotheses to explain the productivity change associated
81 with the mass extinction. An early model was the Strangelove Ocean Hypothesis, which
82 postulated the near complete cessation [*Hsü et al.*, 1982b; *Hsü and McKenzie*, 1985] or reduction
83 [*Zachos et al.*, 1989] of *primary productivity* in the surface ocean leading to reduced export of
84 organic matter to the deep ocean. Carbon cycle modeling showed that it was not necessary for
85 productivity to stop entirely to explain the loss of surface-to-deep $\delta^{13}\text{C}$ gradients; a 10%
86 reduction in the efficiency of the biological pump sufficed [*Kump*, 1991]. More recently,
87 *D'Hondt et al.* [1998] suggested that primary productivity was nearly unchanged by the

88 extinction, but the replacement of large grazers by microbially dominated communities in the
89 surface ocean drastically reduced export production to the sea floor. This hypothesis of a
90 dominant microbial food loop has been called “The Living Ocean Hypothesis” [*D'Hondt et al.*,
91 1998; *D'Hondt*, 2005] because it posits a shift in the way organic production is recycled rather
92 than the reduction of oceanic primary productivity.

93 Both the Living Ocean hypothesis and Strangelove Ocean hypothesis assume that a
94 prolonged (3-4 million years) global decline in export production is responsible for collapsed
95 surface-to-deep $\delta^{13}\text{C}$ gradients [*Hsü and McKenzie*, 1985; *Zachos et al.*, 1989; *D'Hondt et al.*,
96 1998; *D'Hondt*, 2005]. It is therefore surprising that benthic foraminifera did not suffer a mass
97 extinction at the K-Pg boundary [*Culver*, 2003]. Benthic communities are largely dependent on
98 the flux of organic matter from the pelagic realm [*Goody*, 2003], and the lack of extinction in
99 benthic species is paradoxical in light of an apparent global decrease in food supply [*Thomas*,
100 2007]. Many benthic foraminiferal communities do appear to have experienced a period of
101 altered community composition across the K-Pg boundary, suggestive of a decrease in the local
102 food supply [*Widmark and Malmgren*, 1992; *Culver*, 2003; *Alegret and Thomas*, 2005].
103 Surprisingly, this is not true everywhere; at some locales (Figure 1) benthic foraminiferal
104 community structure suggests robust or even increased organic fluxes across the K-Pg boundary
105 [*Alegret and Thomas*, 2009], even in cases where $\delta^{13}\text{C}$ gradients or sedimentation rates suggest
106 reduced export production. In these locations, the robust export productivity to the deep sea
107 suggested by both the lack of species extinctions and the structure of benthic foraminiferal
108 communities directly conflicts with the Living Ocean hypothesis for decreased export
109 productivity from the surface ocean and the standard interpretation of collapsed $\delta^{13}\text{C}$ gradients.
110 Thus, hypotheses for the apparent pelagic-benthic decoupling across the K-Pg boundary include

111 weaker benthic-pelagic coupling in warmer seas [Thomas *et al.*, 2000, although later discounted
112 in Thomas 2007], a more rapid recovery of export productivity from the end-Cretaceous mass
113 extinction than indicated by $\delta^{13}\text{C}$ gradients [Thomas, 2007], and/or the regional maintenance of
114 pre-extinction levels of export productivity [Alegret and Thomas, 2009]. The last two mechanisms
115 require that the collapse and recovery of $\delta^{13}\text{C}$ gradients and other carbonate proxies primarily
116 record processes other than a reduction in the amount of export productivity during this time
117 interval [Thomas, 2007], and calls into question inferred changes in export productivity across
118 the K-Pg boundary based on carbonate proxies alone.

119 Other export productivity proxies have also indicated the maintenance or rapid rebound
120 of organic fluxes after the extinction, providing some support for the benthic foraminiferal
121 patterns. For example, siliceous sediments are commonly associated with productive regions of
122 the ocean so it is notable that New Zealand sites had siliceous blooms through the first million
123 years of the Paleocene, with an order of magnitude increase in diatom to radiolarian (primary
124 producer : consumer) ratios and a conspicuous lack of radiolarian extinctions [Hollis *et al.*,
125 1995]. New Zealand sites also record an increase in “biogenic” barium (associated with sinking
126 organic matter) accompanying the siliceous blooms [Hollis *et al.*, 2003]. In addition,
127 geochemical export productivity proxies including reactive phosphorus and organic carbon
128 content did not decline at the K-Pg boundary at one upwelling site in the western North Atlantic
129 [Blake Nose, Faul *et al.*, 2003], although the $\delta^{13}\text{C}$ gradient collapsed [Quilley *et al.*, 2008].
130 Finally, a very high resolution record of biomarkers (biodegradation resistant sterane and hopane
131 ratios) and $\delta^{13}\text{C}_{\text{organic}}$ and $\delta^{15}\text{N}_{\text{organic}}$ from the Fish Clay, Denmark, detail the initial decline and
132 rapid recovery to pre-boundary levels of algal export productivity and community composition
133 within 100 years of the impact [Sepulveda *et al.*, 2009].

134 Here, we seek to resolve the paradox of conflicting effects of the K-Pg boundary on
135 global surface ocean export productivity as recorded in carbonate productivity proxies (surface-
136 to-deep water $\delta^{13}\text{C}$ gradients, sedimentation rates, and carbonate preservation) and non-carbonate
137 productivity proxies (benthic foraminiferal community structure, biomarkers, and other
138 geochemical proxies like biogenic barium and organic carbon content). We estimate the relative
139 changes in export productivity in multiple ocean basins using biogenic barium. Biogenic barium
140 (Ba_{bio}) is a widely used productivity proxy that correlates well with modern export production
141 [Dymond *et al.*, 1992; Francois *et al.*, 1995; Eagle *et al.*, 2003] and has been used to trace
142 changes in Cenozoic productivity [e.g., Paytan *et al.*, 1996; Thompson and Schmitz, 1997; Bains
143 *et al.*, 2000; Griffith *et al.*, 2010]. We compare our export production records to existing
144 carbonate and non-carbonate paleoproductivity proxy records to test the spatial extent of the
145 Living Ocean Hypothesis.

146

147 **2. METHODS**

148 ***2.1 Biogenic Barium as an Export Productivity Proxy***

149 Marine barite (BaSO_4) is the primary form of biogenic barium (Ba_{bio}) and has a strong,
150 empirical relationship with the export of organic carbon to the deep sea in oxic to suboxic, open
151 ocean sedimentary environments [Dymond *et al.*, 1992; Francois *et al.*, 1995; Eagle *et al.*, 2003;
152 Paytan and Griffith, 2007]. Barite has been found to precipitate in the decaying organic remains
153 of siliceous plankton, phytoplankton, and acantharians [as reviewed in Paytan and Griffith,
154 2007], although the dominant mechanisms by which Ba_{bio} provides a tracer of export
155 productivity are still uncertain. We use the term Ba_{bio} to refer to all barium productivity proxies
156 considered in this study including excess barium ($\text{Ba}_{\text{excess}}$) and Ba/Al, Ba/Ti, and/or Ba/Fe ratios.

157 Barium has both a biogenic source and a terrestrial source. Biogenic barium (Ba_{bio}) can
158 be determined by normalizing the total barium content of sediment to the non-biogenic
159 component (Ba_{detrital}) using a conserved terrestrially sourced tracer such as aluminum (Al) or
160 titanium (Ti) [e.g., *Dymond et al.*, 1992; *Francois et al.*, 1995; *Reitz et al.*, 2004]. Alternatively,
161 Ba_{bio} can be calculated directly by dissolution of other sedimentary components and analysis of
162 the remaining distinctive euhedral crystals of barite formed in sinking organic matter [*Paytan*,
163 1996; *Paytan and Griffith*, 2007]. Ba_{bio} determined by normalization—excess Barium (Ba_{excess})—
164 may deviate widely from those determined with direct barite extraction [e.g., *Dymond et al.*,
165 1992; *Eagle et al.*, 2003]. However, in practice, both methods yield comparable results in
166 calcareous sediments without large diatom, radiolarian or biogenic mud components, with Ba_{bio}
167 levels greater than ~100ppm, and with $Ba_{\text{bio}} \gg Ba_{\text{detrital}}$ [*Eagle et al.*, 2003; *Gonneea and Paytan*,
168 2006]. Ba_{excess} (calculated from sedimentary barium content) and barite (extracted from
169 sediment) must be normalized to accurate sedimentary mass accumulation rates (MARs) to
170 interpret the data in terms of relative or absolute export productivity. The need for accurate MAR
171 introduces a large source of potential error in productivity calculations [*Dymond et al.*, 1992;
172 *Anderson and Winckler*, 2005; *Calvert and Pedersen*, 2007].

173 Ba/Al or Ba/Ti ratios provide an alternate means of inferring export productivity and are
174 not dependent on accurate MAR [*Goldberg and Arrhenius*, 1958; *Murray et al.*, 2000; *Calvert*
175 *and Pedersen*, 2007]. However, different terrestrial sources can contain varying amounts of Ba
176 relative to Ti and Al [*Paytan and Griffith*, 2007] so long-term trends in these ratios could simply
177 reflect changes in the terrestrial sources of barium and other lithogenic elements. For instance,
178 changes in Ba/Al ratios do not always parallel changes in barite and/or Ba_{excess} in Pleistocene
179 sediments [*Averyt and Paytan*, 2004], and it is unclear which proxy most accurately reflects

180 export productivity over this time. The discrepancy between Ba/Al and barite could be due to
181 changes in Ba-depleted dust fluxes affecting Ba/Al ratios [Anderson and Winckler, 2005] or,
182 alternatively, may reflect problems with accurately calculating MAR for barite and Ba_{excess}
183 fluxes [Calvert and Pedersen, 2007]. Here we include and compare both Ba_{excess} (calculated from
184 total sedimentary barium content) and Ba/Al (or Ba/Ti) ratios to account for the differing
185 strengths of each approach. We also consider Ba/Fe ratios in addition to Ba/Al and Ba/Ti ratios,
186 as Fe is better measured by XRF core scanning than Ti and Al and, in certain environments,
187 should also primarily reflect the deposition of terrestrial material.

188 **2.2 Measurement of Biogenic Barium: excess Barium and Barium Ratios**

189 We examined Ba_{excess} (determined by direct measurement of barium concentrations),
190 Ba/Al, Ba/Ti, and/or Ba/Fe at five sites (Figure 1): i) the Vigo Seamount, North Atlantic, Deep
191 Sea Drilling Project (DSDP) Hole 398D, ii) São Paulo Plateau, South Atlantic, DSDP Site 356,
192 iii) Maud Rise, Antarctica, Ocean Drilling Program (ODP) Hole 690C, iv) Shatsky Rise, North
193 Pacific, DSDP Site 577B and ODP Site 1209, and v) Wombat Plateau, Indian Ocean, ODP Hole
194 761C. Age models were derived using shipboard bio- and magnetostratigraphy and the time scale
195 of Berggren *et al.* [1995] (age models provided in Supplemental Tables 5), at all sites except for
196 the Shatsky Rise sites. At Shatsky Rise we used the age model of Westerhold *et al.* [2008] for
197 ODP Site 1209 and tied DSDP Hole 577B to Westerhold *et al.*'s age model for ODP Site 1211
198 using XRF Fe measurements. We shifted Westerhold *et al.*'s age model in both Shatsky Rise
199 sites by 0.28 million years to match the 65 million year age of the K-Pg boundary used by
200 Berggren *et al.* [1995].

201 We used X-ray fluorescence (XRF) measurements at 10 kV and 50 kV to obtain high-
202 resolution records of barium (Ba), iron (Fe) and titanium (Ti) in total counts from DSDP Sites

203 356, 398D, and 577 and ODP Sites 690C and 1209 (Supplemental Tables 1-4). We also use
204 existing Ba, Fe, and Al records from Shatsky Rise [DSDP Site 577, *Michel et al.*, 1985] and the
205 Wombat Plateau [ODP Hole 761C, *Rocchia et al.*, 1992] to calculate Ba/Al, Ba/Fe and Ba_{excess}.
206 Ba_{excess} was calculated according to Dymond [1992] using a detrital barium ratio of 0.0037
207 (determined empirically by Reitz et al. [2004] to be more accurate than the crustal average of
208 0.0075 used by Dymond). The Vigo Seamount and São Paulo Plateau cores were scanned on the
209 Avaatech XRF at the Center for Marine Environmental Science, University Bremen, Germany,
210 and the Maud and Shatsky cores on the Avaatech XRF at Scripps Institution of Oceanography
211 Geological Collections. We collected XRF data every centimeter over the intervals shown
212 (Figure 3), using a 1 cm² footprint and 30 second count time for 10kV and 50kV respectively
213 (see Supplemental Tables 1-4 for site and core specific μ A settings). XRF measurements are
214 reported as total counts and, without empirical standardization, can only be used to calculate
215 elemental ratios (Ba/Ti and Ba/Fe) not Ba_{excess}. Notably, Ba/Ti XRF measurements have been
216 used in previous paleoproductivity studies and shown to correlate very well with quantitative
217 ICPMS measurements [*Jaccard et al.*, 2009; *Jaccard et al.*, 2010]. We compared our XRF Ba
218 and Ti measurements against quantitative Ba and Al measurements for DSDP Hole 577B,
219 Shatsky Rise (Figure 4), and obtained qualitatively similar trends in spite of extensive core aging
220 (recrystallization, reprecipitation, mold, and desiccation). Al was poorly detected by XRF in our
221 carbonate rich, deep sea sediments so we use Fe and Ti counts to normalize our XRF
222 measurements of Ba. As cores were measured on different machines and with different
223 instrument settings, the ratio of Ba/Ti can only be considered within a given site; absolute ratio
224 values cannot be compared across sites without quantitative measurements.

225

225 **2.3 Ba_{bio} Preservation Considerations**

226 General site characteristics at all sites suggest that biogenic barium should be well
227 preserved: all sites are biostratigraphically complete within the boundary sections examined here,
228 are comprised of nannofossil oozes to chalks with minor amounts of biogenic silica, and have
229 evidence of oxic depositional environments including bioturbated K-Pg boundaries and pale tan
230 to reddish boundary sediments [*Perch-Nielsen et al.*, 1977; *Ryan and al.*, 1979; *Moore et al.*,
231 1984; *Heath et al.*, 1985; *Barker et al.*, 1988; *Bralower et al.*, 2002]. We considered, but did not
232 include, barium proxies at DSDP Site 527, Walvis Ridge, South Atlantic as this site had a
233 relatively high proportion of detrital to biogenic barium (20-100% detrital). In cores with high
234 detrital barium, small changes in source Ba and Al composition can dramatically affect the
235 calculated Ba_{excess} or Ba/Al, thereby precluding the use of Ba_{excess} or Ba/Al for inferences about
236 productivity [*Dymond et al.*, 1992; *Reitz et al.*, 2004].

237 **2.4 Productivity Proxy Compilation**

238 We compare our results with published accounts of early Paleocene primary productivity
239 from studies of benthic foraminifera and non-carbonate geochemical proxies. We restrict our
240 comparison to a small subset of the available benthic foraminiferal proxy records, choosing the
241 taxonomic and stratigraphic stability of a single research group over the extensive coverage
242 offered by considering studies from the entire literature. In studies of benthic foraminiferal
243 community structure, the increased ratios of infaunal to epifaunal forms, buliminid taxa, and
244 Benthic Foraminiferal Accumulation Rates (BFAR) can be indicative of increased influxes of
245 export production to the seafloor [e.g., *Goody, 2003; Jorissen et al.*, 2007]. Therefore, the
246 benthic foraminiferal proxies summarized by our map (Figure 1) represent the dominant
247 conclusions based on infaunal to epifaunal ratios and the proportion of buliminid taxa reached by

248 Alegret, Thomas, and others at the following 16 sites: Mexican Sites (Los Ramones, El Penon,
249 El Tecolote, La Ceiba, El Mulato, La Lajila, El Mimbral, and Coxquihui) [Alegret *et al.*, 2001;
250 Alegret and Thomas, 2001; Alegret *et al.*, 2002]; Blake Nose, east of Florida [Alegret and
251 Thomas, 2005]; Agost, Spain [Alegret *et al.*, 2003]; Loya, Spain [Alegret, 2007]; Bidart, France
252 [Alegret *et al.*, 2004]; Aïn Settara, Tunisia [Peryt *et al.*, 2002]; Walvis Ridge, eastern South
253 Atlantic [Alegret and Thomas, 2007]; Maud Rise, Antarctica [Thomas, 1990]; Hess Rise, North
254 Pacific [Alegret and Thomas, 2009]; and Shatsky Rise, North Pacific [Alegret and Thomas,
255 2009]. We limit our discussion of this body of work to conclusions regarding the relative amount
256 of organic matter reaching the seafloor. It is notable, however, that these studies also discuss the
257 temporal stability and relative quality of the export production, generally finding decreased
258 stability and/or food quality in the earliest Danian even in sites lacking evidence of declines in
259 total export production. We also consider the results and interpretations of three geochemical
260 studies: Blake Nose, east of Florida, using reactive P and organic C [Faul *et al.*, 2003];
261 Marlborough, New Zealand, using biogenic barium, excess silica, and diatom/radiolarian ratio
262 proxies [Hollis *et al.*, 1995; Hollis *et al.*, 2003]; and the Fish Clay, Denmark, using sterane and
263 hopane biomarkers, and $\delta^{13}\text{C}_{\text{organic}}$ and $\delta^{15}\text{N}_{\text{organic}}$ [Sepulveda *et al.*, 2009].

264

265 **3. RESULTS AND DISCUSSION**

266 ***3.1 K-Pg Boundary Related Changes in Export Productivity***

267 Proxy data suggests that the K-Pg extinction did not affect export production the same
268 way in all ocean basins or habitats (Figure 1; heterogeneous benthic patterns previously
269 discussed in [e.g., Culver, 2003; Alegret and Thomas, 2005; 2007; 2009] and $\delta^{13}\text{C}$ in [Meyers
270 and Simoneit, 1990; Stott and Kennett, 1990]). These results contrast with a previous synthesis

271 [D'Hondt, 2005], which found global declines in export productivity based on carbonate proxies
272 (e.g., surface-to-deep water $\delta^{13}\text{C}$ gradients, sedimentation rates, and carbonate preservation).

273 We find a decrease in export productivity coincident with the K-Pg boundary in the
274 Atlantic (Vigo and São Paulo), Antarctic (Maud), and Indian (Wombat) Oceans (Figure 2) using
275 barium proxies ($\text{Ba}_{\text{excess}}$, Ba/Al , Ba/Ti , and Ba/Fe) of organic flux to the deep sea. At Maud Rise,
276 Ba/Ti and Ba/Al ratios recover to pre-impact levels within ~ 350 kyr, supporting the rapid
277 resurgence in export productivity previously hypothesized on the basis of surface to deep $\delta^{13}\text{C}$
278 gradients [Stott and Kennett, 1989, using same age model]. In contrast, barium proxies and
279 inferred organic fluxes fail to recover over the interval studied at São Paulo, Wombat, and
280 Vigo—a period of more than 600 kyr at Sao Paulo and Wombat (Figure 2) and more than 2
281 million years at Vigo (Figure 3).

282 At Shatsky Rise in the Pacific, barium proxies are somewhat ambiguous due to
283 differences between Ba/Al , Ba/Fe , and $\text{Ba}_{\text{excess}}$ at DSDP Site 577B and Ba/Ti and Ba/Fe at ODP
284 Site 1209 (Figure 2e-f), but provide no evidence for a distinct, prolonged K-Pg-associated
285 decline in export productivity. At DSDP Hole 577B, Ba/Al ratios and $\text{Ba}_{\text{excess}}$ actually increase
286 sharply in the very earliest Danian, supporting inferences of increased export production based
287 on benthic foraminifera proxies at Shatsky Rise (ODP Site 1210) and Hess Rise (DSDP Site 465)
288 [Alegret and Thomas, 2009] and a sparse $\delta^{13}\text{C}_{\text{organic}}$ record from Shatsky Rise [Meyers and
289 Simoneit, 1990]. XRF Ba/Ti measurements also increase sharply at DSDP Hole 577B and match
290 Ba/Al results in expressing a longer duration excursion of elevated export productivity than
291 revealed by $\text{Ba}_{\text{excess}}$ (Figure 4). Ba/Fe ratios are unchanged or increase slightly across the K-Pg
292 boundary at both DSDP Hole 577B and ODP Site 1209, but diverge from measurements of Ba/Ti
293 and Ba/Al in the same site. Ba/Ti decreases slightly across the boundary at ODP Site 1209, but is

294 well within the range of pre-boundary oscillations and exceeds pre-boundary export productivity
295 fluxes within ~300 kyr. We regard our measurements of Ba/Ti with some skepticism at ODP
296 Site 1209 during this interval given XRF limitations in measuring the very low Ti concentrations
297 in these sediments. When considered together, the best proxies at each Shatsky Rise site support
298 either no change (Ba/Fe ratios at ODP Site 1209) or a short, ~100 kyr burst in export production
299 in the North Pacific (Ba/Al, Ba/Ti, and Ba_{bio} at DSDP Hole 577B and benthic foraminifera
300 proxies at ODP Site 1210).

301 The sites investigated to date using barium, benthic foraminifera, and other geochemical
302 proxies indicate differences in biotic responses by geography and habitat. At the largest scale,
303 organic fluxes at sites in the Pacific appear to be maintained or increased in the earliest Danian,
304 while most sites in the North Atlantic show large, persistent declines in export production
305 (Figure 1). This global heterogeneity does not appear to be a proxy artifact. Both benthic
306 foraminifera and barium proxies in North Atlantic and Tethyan sites near Vigo Seamount (e.g.,
307 Loya, Bidart, Agost and Aïn Settara) show boundary declines, while both benthic foraminifera
308 and barium in North Pacific sites at Shatsky and Hess Rise support maintained to increased
309 organic fluxes in the very earliest Danian.

310 The pattern in the South Atlantic is more complex. At Walvis Ridge, in the eastern South
311 Atlantic, benthic foraminifera proxies indicate no change in total export production across the
312 boundary [*Alegret and Thomas, 2007*]. Conversely, there is a large drop in export production
313 measured by Ba/Ti at São Paulo, in the western South Atlantic. A drop in export production is
314 also indicated at Maud Rise, near Antarctica, by benthic foraminifer (low resolution) and barium
315 proxies. However, the export productivity decline at Maud Rise is within the scope of pre-
316 boundary oscillations (Figure 2c) and is reversed and surpassed about 350 kyr after the

317 extinction. From this limited sample size, it is unclear whether South Atlantic sites are generally
318 less affected by boundary events than the North Atlantic, or if this pattern merely reflects the
319 chance sampling of a few relatively unaffected sites in a region characterized by K-Pg-related
320 declines in export production.

321 Most sites in the North Atlantic indicate large K-Pg related declines in export
322 productivity, with a few notable exceptions. Export productivity was relatively unaffected by the
323 K-Pg boundary events at Blake Nose, in the western North Atlantic, and the Fish Clay, Denmark
324 in contrast to most North Atlantic sites [*Faul et al.*, 2003; *Alegret and Thomas*, 2005; *Sepulveda*
325 *et al.*, 2009]. Benthic foraminifera proxies at Blake Nose –hypothesized to have been located in a
326 productive, coastal upwelling region– indicate a short, ~100,000 year decline in export
327 productivity in the early Paleocene [*Alegret and Thomas*, 2005]. This brief decline in export
328 productivity is not captured by the relatively low-resolution geochemical proxy record of *Faul et*
329 *al.*[2003] which records no affect of the K-Pg boundary on export productivity. Similarly, the
330 Fish Clay is a neritic site and has a very brief, decadal-scale decline in productivity as indicated
331 by biomarkers [*Sepulveda et al.*, 2009]. We represent the Fish Clay site as roughly unaffected by
332 the K-Pg boundary in regards to export productivity (Fig. 1) as the decline and recovery in
333 biomarkers spans a much shorter temporal scale than can be resolved in the deep sea.

334 Export productivity in the modern ocean varies between habitats, with the proportion of
335 productivity exported from the surface ocean ranging from around 5-60% of total surface
336 productivity [*Laws et al.*, 2000; *Dunne et al.*, 2005], and corresponding to concordant differences
337 in temperature, primary productivity, and community structure, among others. The K/Pg
338 collapse of surface to deep $\delta^{13}\text{C}$ gradients in sites throughout the global ocean suggested a
339 prolonged decrease in export productivity across oceanic environments with different

340 background levels of export productivity and ecological structure. Our results support a more
341 heterogeneous pattern of export changes, with different oceanic regions varying in the
342 magnitude, direction, and duration of export productivity change.

343 One existing hypothesis for the spatially heterogeneous response of benthic foraminiferal
344 export proxies is that the response of individual locales is related to differences in habitat type
345 [e.g., *Culver*, 2003; *Alegret and Thomas*, 2005; 2007; 2009]. This could arise, for instance, if
346 post-extinction communities in highly productive, temporally variable environments rebounded
347 much more rapidly from the K-Pg impact due to the ecological similarity of early Danian species
348 to some pre-extinction nearshore species [*D'Hondt et al.*, 1996]. Indeed, early Paleocene bloom
349 taxa in planktonic foraminifera are descendants of coastal taxa in the late Maastrichtian and
350 therefore may have been adapted to the generally high productivity and temporal variability of
351 coastal waters [*MacLeod*, 1993; *D'Hondt et al.*, 1996].

352 However, the habitat-type related hypothesis appears to only partially capture the
353 variability of the direction, magnitude, and duration of export productivity change. For instance,
354 there is some evidence that export productivity in coastal and upwelling sites was generally
355 unaffected or rapidly recovered (Fish Clay and Blake Nose, North Atlantic) or even increased by
356 the K-Pg mass extinction (New Zealand sites) [e.g., *Culver*, 2003; *Alegret and Thomas*, 2005;
357 2007; 2009]. This pattern is countered, however, by the response of other coastal sites that do
358 experience a period of depressed export production (e.g., Aïn Settara, Agost, Bidart). In addition,
359 the two most open ocean, oligotrophic sites in the study –Hess Rise and Shatsky Rise, North
360 Pacific– indicate a brief burst of export productivity, the opposite of the expected habitat effect
361 as described above. Other environmental factors like the proportion of calcareous to siliceous
362 primary producers also do not appear to explain the boundary change in export productivity. The

363 most carbonate dominated (Shatsky Rise) and siliceous dominated (New Zealand) sites both
364 exhibited an early burst in export productivity despite dramatic differences in extinction of
365 dominant fossilized primary producers and consumers.

366 We similarly do not find support for the hypothesized hemispherical effect of the K-Pg
367 impact [*Jiang et al.*, 2010], which suggested a delayed recovery in northern hemisphere sites
368 relative to southern hemisphere sites due to impact-related heavy metal poisoning. Some sites
369 with an early Paleocene export productivity burst (Shatsky and Hess Rise, North Pacific) or with
370 relatively unaffected export productivity (Fish Clay, Denmark) are in the northern hemisphere.
371 Conversely, some southern hemisphere sites have decreased, rather than increased, export
372 productivity (São Paulo, Wombat). The distance from the impactor (shown to be important for
373 recovery of nearly coastal mollusks [*Jablonski*, 1998]) also appears unrelated to the change in
374 export productivity, with relatively unaffected or rapidly recovered sites (Fish Clay, Denmark
375 and Blake Nose, South Atlantic) equal or closer to the impact site than sites with strongly
376 depressed export productivity (e.g., Vigo Seamount).

377 A change in circulation, weathering, and/or stratification [the first two as proposed in
378 *Alegret and Thomas*, 2009] could drive a spatially heterogeneous change in export productivity.
379 However, there is no evidence for regional changes in any of these three drivers at the K-Pg
380 boundary, and it is unclear what could drive and maintain regional changes in circulation,
381 weathering, or stratification for up to 2-million years. Regional variation in the extinction
382 intensity and recovery of un- or poorly fossilized marine groups offers an equally speculative
383 hypothesis for the spatially heterogeneous changes in export productivity. In sum, we find
384 evidence against a number of potential drivers of the spatial and temporal heterogeneity of export
385 productivity change –including habitat type, dominant primary producer, hemispherical impactor

386 effects, distance from the impactor. Other plausible scenarios currently lack positive support and
387 include heterogeneity in the K-Pg response of circulation, weathering, stratification, or the
388 extinction and recovery of unfossilized marine species. Insight into the mechanisms driving the
389 spatial and temporal heterogeneity of export productivity change across the K-Pg boundary thus
390 awaits further empirical and theoretical research.

391

392 ***3.2 The K-Pg Impact and the Fidelity of Carbonate Productivity Proxies***

393 An apparent global collapse in export productivity indicated by the surface-to-deep $\delta^{13}\text{C}$
394 gradient contradicts benthic foraminiferal and non-carbonate geochemical proxies in the Pacific
395 and some Atlantic sites (Fig.1, 2). In these locations, processes other than export productivity
396 must dominate the signal in one or more of the productivity proxies. We highlight several
397 biological and biogeochemical effects of the K-Pg impact and extinction that may affect the
398 fidelity of carbonate productivity proxies in the early Paleocene.

399 The K-Pg impact lead to the extinction of nearly all species of the dominant surface
400 ocean carbonate producers, including the calcareous nannoplankton and the planktonic
401 foraminifera, with direct biological and ecological effects on $\delta^{13}\text{C}$ values [e.g., *Berggren and*
402 *Norris, 1997; Minoletti et al., 2005; Paytan, 2008; Alegret and Thomas, 2009*]. Early Paleocene
403 nannoplankton assemblages are dominated by otherwise rare calcareous dinoflagellate cysts
404 (*Thoracosphaera*) that have distinctly light, or more benthic-like, $\delta^{13}\text{C}$ signatures [*Minoletti et*
405 *al., 2005*]. The planktonic foraminifera that diversified in the early Paleocene also had relatively
406 negative $\delta^{13}\text{C}$ signatures compared to late Cretaceous species, an observation consistent with a
407 lack of photosymbionts, a deep depth habitat, and a small test size [*Berggren and Norris, 1997;*
408 *Bornemann and Norris, 2007*]. Together, biological and ecological changes in pelagic carbonate

409 producers at the K-Pg may have had a large effect on planktonic $\delta^{13}\text{C}$ values, shifting the ratio
410 towards more negative values independent of a change in export production.

411 Sedimentation rates of calcite and biogenic opal can provide a proxy for changes in
412 export productivity when the relationship between fossilized and unfossilized groups is constant
413 [Paytan, 2008], an assumption that does not appear to hold following the end-Cretaceous
414 extinction. A decrease in nannoplankton (primarily coccolithophorid) sedimentation does not
415 necessarily indicate a decrease in global primary production [Alegret and Thomas, 2009].
416 Modern coccolithophorids are poor competitors in unstable, variable environments [Litchman,
417 2007], and benthic foraminiferal assemblages suggest that such conditions characterized early
418 Paleocene seas [Alegret and Thomas, 2007]. Furthermore, there is evidence that other primary
419 producers such as diatoms in New Zealand and naked algae in Denmark may have had increased
420 population sizes in response to K-Pg boundary environmental and ecological perturbations
421 [Hollis et al., 1995; Hollis et al., 2003; Sepulveda et al., 2009]. In addition, the decrease in
422 sedimentation rates at the K-Pg boundary is predominantly driven by decreased nannoplankton
423 sedimentation [D'Hondt, 2005], with an increase in coarse carbonate fractions in the early
424 Paleocene [Zachos and Arthur, 1986; Zachos et al., 1989; Bralower et al., 2010].

425

426 4. CONCLUSIONS

427 The end-Cretaceous mass extinction temporarily changed the global geography of the
428 export of organic matter from the surface ocean to the deep sea; some regions had profound
429 reductions in export productivity that persisted for up to 2-million years, while others were
430 characterized by constant or rapidly re-established organic flux from the surface ocean to the
431 deep sea floor. A globally and temporally heterogeneous response of export productivity is in

432 keeping with the highly regional responses of ecosystems in other environments –terrestrial,
433 shallow marine, and near coastal– to the K-Pg boundary events [*Hollis et al.*, 1995; *Jablonski*,
434 1998; *Stilwell*, 2003; *Wilf and Johnson*, 2004; *Sepulveda et al.*, 2009; *Wappler et al.*, 2009], but
435 challenges the Living Ocean Hypothesis which posits a global response on the bases of carbonate
436 proxies.

437 Our study demonstrates the utility of barium proxies for quantifying changes in export
438 productivity during events when proxies like carbonate $\delta^{13}\text{C}$ or sedimentation rate may be
439 affected by biological factors like extinction and ecological change. We find general
440 concordance between non-carbonate geochemical proxies for export productivity –like barium–
441 and the response of benthic foraminiferal community structure, suggesting that carbonate proxies
442 may record other changes in factors other than (or in addition to) local export productivity during
443 this interval.

444 More generally, our results highlight the need for multiproxy, multi-site studies to
445 quantify the response of the global ocean to massive perturbations. At present it is not clear what
446 mechanisms are responsible for the temporal heterogeneity in the recovery of export productivity
447 to pre-extinction levels or for the spatial heterogeneity in the magnitude and direction of change.
448 Additional multiproxy records from other locations are needed in order to develop a robust
449 model that can account for the temporal and regional heterogeneity of organic flux change at the
450 K-Pg boundary. Generalizing the response of the ocean, or even of an ocean basin, to the K-Pg
451 mass extinction on the basis of a single or a few sites is not suggested at present given the lack of
452 mechanistic understanding for the observed spatial heterogeneity in export productivity change.

453

453 **ACKNOWLEDGEMENTS**

454 We gratefully acknowledge the generous help of A. Hangsterfer (SIO Geological
455 Collections Manager), and S. van der Gaast (Avaatech) and A. Vaars (Avaatech) for scanning
456 support at Scripps Institution of Oceanography; S. Kirtland (SIO), T. Westerhold, and U. Röhl
457 for scanning at the Bremen Core Repository; P. Rumford, J. Firth and many others at the Gulf
458 Coast Repository for core shipping and scanning discussions; and J. Carilli, K. Cramer, M.
459 Forrest, P. Franks, M. Ohman and S. Kirtland for thoughtful comments and suggestions. We
460 thank the two reviewers, Adina Paytan and Laia Alegret, and editor, Rainer Zahn, for through
461 and thoughtful reviews that substantially improved the clarity of the manuscript. This work was
462 supported by a NASA Exobiology grant NNX07AK62G and made possible by the Ocean
463 Drilling Program.

464

464 **REFERENCES**

- 465
- 466 Alegret, L. (2007), Recovery of the deep-sea floor after the Cretaceous-Paleogene boundary
 467 event: The benthic foraminiferal record in the Basque-Cantabrian basin and in South-eastern
 468 Spain, *Palaeogeography Palaeoclimatology Palaeoecology*, 255(1-2), 181-194.
- 469 Alegret, L., and E. Thomas (2001), Upper Cretaceous and lower Paleogene benthic foraminifera
 470 from northeastern Mexico, *Micropaleontology*, 47(4), 269-316.
- 471 Alegret, L., and E. Thomas (2005), Cretaceous/Paleogene boundary bathyal paleo-environments
 472 in the central North Pacific (DSDP Site 465), the Northwestern Atlantic (ODP Site 1049), the
 473 Gulf of Mexico and the Tethys: the benthic foraminiferal record, *Palaeogeography*
 474 *Palaeoclimatology Palaeoecology*, 224(1-3), 53-82.
- 475 Alegret, L., and E. Thomas (2007), Deep-sea environments across the Cretaceous/Paleogene
 476 boundary in the eastern South Atlantic Ocean (ODP leg 208, Walvis ridge), *Marine*
 477 *Micropaleontology*, 64(1-2), 1-17.
- 478 Alegret, L., and E. Thomas (2009), Food supply to the seafloor in the Pacific Ocean after the
 479 Cretaceous/Paleogene boundary event, *Marine Micropaleontology*, 73, 105-116.
- 480 Alegret, L., E. Molina, and E. Thomas (2001), Benthic foraminifera at the Cretaceous-Tertiary
 481 boundary around the Gulf of Mexico, *Geology*, 29(10), 891-894.
- 482 Alegret, L., E. Molina, and E. Thomas (2003), Benthic foraminiferal turnover across the
 483 Cretaceous/Paleogene boundary at Agost (southeastern Spain): paleoenvironmental inferences,
 484 *Marine Micropaleontology*, 48(3-4), 251-279.
- 485 Alegret, L., M. A. Kaminski, and E. Molina (2004), Paleoenvironmental recovery after the
 486 Cretaceous/Paleogene boundary crisis: evidence from the marine bidart section (SW France),
 487 *Palaios*, 19(6), 574-586.
- 488 Alegret, L., I. Arenillas, J. A. Arz, and E. Molina (2002), Environmental changes triggered by
 489 the K/T impact event at Coxquihui (Mexico) based on foraminifera, *Neues Jahrbuch Fur*
 490 *Geologie Und Palaontologie-Monatshefte*(5), 295-309.
- 491 Anderson, R. F., and G. Winckler (2005), Problems with paleoproductivity proxies,
 492 *Paleoceanography*, 20(3).
- 493 Averyt, K. B., and A. Paytan (2004), A comparison of multiple proxies for export production in
 494 the equatorial Pacific, *Paleoceanography*, 19(4).
- 495 Bains, S., R. D. Norris, R. M. Corfield, and K. L. Faul (2000), Termination of global warmth at
 496 the Palaeocene/Eocene boundary through productivity feedback, *Nature*, 407(6801), 171-174.
- 497 Barker, P. F., J. P. Kennett, and e. al. (1988), Site 690, in *Proc. ODP, Init. Repts., 113*, edited by
 498 P. F. Barker, J. P. Kennett and e. al., pp. 183-292, Ocean Drilling Program, College Station, TX.

- 499 Berggren, W. A., and R. D. Norris (1997), Biostratigraphy, phylogeny and systematics of
500 Paleocene trochospiral planktic foraminifera, *Micropaleontology*, 43, 1-116.
- 501 Berggren, W. A., D. V. Kent, C. C. Swisher, and M.-P. Aubry (1995), *Geochronology, time*
502 *scales and global stratigraphic correlation*, *SEPM Special Publication 54*, 1-386 pp., SEPM,
503 Tulsa.
- 504 Bornemann, A., and R. D. Norris (2007), Size-related stable isotope changes in Late Cretaceous
505 planktic foraminifera: Implications for paleoecology and photosymbiosis, *Marine*
506 *Micropaleontology*, 65(1-2), 32-42.
- 507 Bralower, T., I. Premoli Silva, M. J. Malone, and e. al. (2002), Site 1209, in *Proc. ODP, Initial*
508 *Reports, 198*, edited by T. Bralower, I. Premoli Silva and M. J. Malone, pp. 1-102, Ocean
509 Drilling Program, College Station, TX.
- 510 Bralower, T., L. Eccles, J. Kutz, T. Yancey, J. Schueth, M. Arthur, and D. Bice (2010), Grain
511 size of Cretaceous-Paleogene boundary sediments from Chicxulub to the open ocean:
512 Implications for interpretation of the mass extinction event, *Geology*, 38(3), 199-202.
- 513 Calvert, S. E., and T. F. Pedersen (2007), Elemental proxies for palaeoclimatic and
514 palaeoceanographic variability in marine sediments: interpretation and application, in *Proxies in*
515 *late Cenozoic paleoceanography*, edited by C. Hillaire-Marcel and A. de Vernal, pp. 567-644,
516 Elsevier, Oxford.
- 517 Coxall, H. K., S. D'Hondt, and J. C. Zachos (2006), Pelagic evolution and environmental
518 recovery after the Cretaceous-Paleogene mass extinction, *Geology*, 34(4), 297-300.
- 519 Culver, S. J. (2003), Benthic foraminifera across the Cretaceous-Tertiary (K-T) boundary: a
520 review, *Marine Micropaleontology*, 47(3-4), 177-226.
- 521 D'Hondt, S. (2005), Consequences of the Cretaceous/Paleogene mass extinction for marine
522 ecosystems, *Annual Review of Ecology Evolution and Systematics*, 36, 295-317.
- 523 D'Hondt, S., P. Donaghay, J. C. Zachos, D. Luttenberg, and M. Lindinger (1998), Organic
524 carbon fluxes and ecological recovery from the Cretaceous-Tertiary mass extinction, *Science*,
525 282(5387), 276-279.
- 526 D'Hondt, S. L., T. D. Herbert, J. King, and C. Gibson (1996), Planktic foraminifera, asteroids
527 and marine production: death and recovery at the Cretaceous-Tertiary boundary, in *The*
528 *Cretaceous-Tertiary event and other catastrophes in Earth history: Geological Society of*
529 *America Special Paper 307*, edited by G. Ryder, D. Fastovsky and S. Gartner, pp. 303-317.
- 530 Dunne, J. P., R. A. Armstrong, A. Gnanadesikan, and J. L. Sarmiento (2005), Empirical and
531 mechanistic models for the particle export ratio, *Global Biogeochemical Cycles*, 19(4), -.
- 532 Dymond, J., E. Suess, and M. Lyle (1992), Barium in deep-sea sediment: a geochemical proxy
533 for paleoproductivity, *Paleoceanography*, 7(2), 163-181.

- 534 Eagle, M., A. Paytan, K. R. Arrigo, G. van Dijken, and R. W. Murray (2003), A comparison
535 between excess barium and barite as indicators of carbon export, *Paleoceanography*, 18(1), 1-13.
- 536 Faul, K. L., L. D. Anderson, and M. L. Delaney (2003), Late Cretaceous and early Paleogene
537 nutrient and paleoproductivity records from Blake Nose, western North Atlantic Ocean,
538 *Paleoceanography*, 18(2), 1-16.
- 539 Francois, R., S. Honjo, S. J. Manganini, and G. E. Ravizza (1995), Biogenic barium fluxes to the
540 deep-sea - implications for paleoproductivity reconstruction, *Global Biogeochemical Cycles*,
541 9(2), 289-303.
- 542 Goldberg, E. D., and G. O. S. Arrhenius (1958), Chemistry of pacific pelagic sediments,
543 *Geochimica Et Cosmochimica Acta*, 13(2-3), 153-212.
- 544 Gonneea, M. E., and A. Paytan (2006), Phase associations of barium in marine sediments,
545 *Marine Chemistry*, 100(1-2), 124-135.
- 546 Gooday, A. J. (2003), Benthic foraminifera (protista) as tools in deep-water palaeoceanography:
547 Environmental influences on faunal characteristics, *Advances in Marine Biology*, 46, 1-90.
- 548 Griffith, E., M. Calhoun, E. Thomas, K. Averyt, A. Erhardt, T. Bralower, M. Lyle, A. Olivarez-
549 Lyle, and A. Paytan (2010), Export productivity and carbonate accumulation in the Pacific Basin
550 at the transition from a greenhouse to icehouse climate (late Eocene to early Oligocene),
551 *Paleoceanography*, 25.
- 552 Heath, G. R., L. H. Burckle, and e. al. (1985), Site 577, in *Init. Repts. DSDP*, 86, edited by G. R.
553 Heath, L. H. Burckle and e. al., pp. 91-137, U.S. Govt. Printing Office, Washington.
- 554 Hollis, C. J., K. A. Rodgers, and R. J. Parker (1995), Siliceous plankton bloom in the earliest
555 tertiary of Marlborough, New-Zealand, *Geology*, 23(9), 835-838.
- 556 Hollis, C. J., C. P. Strong, K. A. Rodgers, and K. M. Rogers (2003), Paleoenvironmental changes
557 across the Cretaceous/Tertiary boundary at Flaxbourne River and Woodside Creek, eastern
558 Marlborough, New Zealand, *New Zealand Journal of Geology and Geophysics*, 46(2), 177-197.
- 559 Hsü, K. J., and A. McKenzie (1985), A “Strangelove” ocean in the earliest Tertiary, in *The*
560 *Carbon Cycle and Atmospheric CO₂: Natural Variations Archean to Present* edited by E. T.
561 Sundquist and W. S. Broecker, pp. 487– 492, American Geophysical Union, Washington, D. C.
- 562 Hsü, K. J., Q. X. He, and A. McKenzie (1982a), Terminal Cretaceous environmental and
563 evolutionary changes, in *Geological implications of impacts of large asteroid and comets on the*
564 *Earth: Geological Society of America Special Paper 190*, edited by L. T. Silver and P. H.
565 Schultz, pp. 317–328.
- 566 Hsü, K. J., et al. (1982b), Mass Mortality and Its Environmental and Evolutionary Consequences,
567 *Science*, 216(4543), 249-256.

- 568 Jablonski, D. (1998), Geographic variation in the molluscan recovery from the end-Cretaceous
569 extinction, *Science*, 279(5355), 1327-1330.
- 570 Jaccard, S. L., E. D. Galbraith, D. M. Sigman, and G. H. Haug (2010), A pervasive link between
571 Antarctic ice core and subarctic Pacific sediment records over the past 800 kyrs, *Quaternary*
572 *Science Reviews*, 29(1-2), 206-212.
- 573 Jaccard, S. L., E. D. Galbraith, D. M. Sigman, G. H. Haug, R. Francois, T. F. Pedersen, P.
574 Dulski, and H. R. Thierstein (2009), Subarctic Pacific evidence for a glacial deepening of the
575 oceanic respired carbon pool *Earth and Planetary Science Letters*, 277, 156-166.
- 576 Jiang, S. J., T. J. Bralower, M. E. Patzkowsky, L. R. Kump, and J. D. Schueth (2010),
577 Geographic controls on nanoplankton extinction across the Cretaceous/Palaeogene boundary,
578 *Nature Geoscience*, 3(4), 280-285.
- 579 Jorissen, F. J., C. Fontanier, and E. Thomas (2007), Paleooceanographical proxies based on deep-
580 sea benthic foraminiferal assemblage characteristics. , in *Proxies in Late Cenozoic*
581 *Paleoceanography: Biological tracers and biomarkers*, edited by C. Hillaire-Marcel and A. de
582 Vernal, Elsevier, Amsterdam.
- 583 Kump, L. R. (1991), Interpreting Carbon-Isotope Excursions - Strangelove Oceans, *Geology*,
584 19(4), 299-302.
- 585 Laws, E. A., P. G. Falkowski, W. O. Smith, H. Ducklow, and J. J. McCarthy (2000),
586 Temperature effects on export production in the open ocean, *Global Biogeochemical Cycles*,
587 14(4), 1231-1246.
- 588 Litchman, E. (2007), Resource competition and the ecological success of phytoplankton, in
589 *Evolution of primary producers in the sea*, edited by P. G. Falkowski and A. H. Knoll, pp. 351-
590 376, Elsevier, Amsterdam.
- 591 MacLeod, N. (1993), The Maastrichtian-Danian radiation of triserial and biserial planktic
592 foraminifera - testing phylogenetic and adaptational hypotheses in the (micro) fossil record,
593 *Marine Micropaleontology*, 21(1-3), 47-100.
- 594 Meyers, P. A., and B. R. T. Simoneit (1990), Global comparisons of organic matter in sediments
595 across the Cretaceous-Tertiary boundary, *Organic Geochemistry*, 16(4-6), 641-648.
- 596 Michel, H. V., F. Asaro, W. Alvarez, and L. W. Alvarez (1985), Elemental profile of iridium and
597 other elements near the Cretaceous/Tertiary boundary in Hole 577B, in *Init. Repts. DSDP*, 86,
598 edited by G. R. Heath, L. H. Burckle and e. al., pp. 533-538, U. S. Govt. Printing Office,
599 Washington.
- 600 Miller, K. G., R. M. Sherrell, J. V. Browning, M. P. Field, W. Gallagher, R. K. Olsson, P. J.
601 Sugarman, S. Tuorto, and H. Wahyudi (2010), Relationship between mass extinction and iridium
602 across the Cretaceous-Paleogene boundary in New Jersey, *Geology*, 38(10), 867-870.

- 603 Minoletti, F., M. de Rafelis, M. Renard, S. Gardin, and J. Young (2005), Changes in the pelagic
604 fine fraction carbonate sedimentation during the Cretaceous-Paleocene transition: contribution of
605 the separation technique to the study of Bidart section, *Palaeogeography Palaeoclimatology*
606 *Palaeoecology*, 216(1-2), 119-137.
- 607 Moore, T. C., Jr., P. D. Rabinowitz, and e. al. (1984), Site 527, in *Init. Repts. DSDP, 74*, edited
608 by T. C. Moore, Jr., P. D. Rabinowitz and e. al., U.S. Govt. Printing Office, Washington.
- 609 Murray, R. W., C. Knowlton, M. Leinen, A. C. Mix, and C. H. Polsky (2000), Export production
610 and carbonate dissolution in the central equatorial Pacific Ocean over the past 1 Myr,
611 *Paleoceanography*, 15(6), 570-592.
- 612 Paytan, A. (1996), Marine barite: A recorder of oceanic chemistry, productivity and circulation,
613 University of California, San Diego, La Jolla, CA.
- 614 Paytan, A. (2008), Ocean paleoproductivity, in *Encyclopedia of Paleoclimatology and Ancient*
615 *Environments*, edited by V. Gornitz, pp. 643-651, Kluwer Academic Publishers.
- 616 Paytan, A., and E. M. Griffith (2007), Marine barite: Recorder of variations in ocean export
617 productivity, *Deep-Sea Research Part II-Topical Studies in Oceanography*, 54(5-7), 687-705.
- 618 Paytan, A., M. Kastner, and F. P. Chavez (1996), Glacial to interglacial fluctuations in
619 productivity in the equatorial Pacific as indicated by marine barite, *Science*, 274(5291), 1355-
620 1357.
- 621 Perch-Nielsen, K., P. R. Supko, and e. al (1977), Site 356: São Paulo Plateau, in *Init. Repts.*
622 *DSDP, 39*, edited by P. R. Supko, K. Perch-Nielsen and e. al, pp. 141-230, U.S. Govt. Printing
623 Office, Washington.
- 624 Peryt, D., L. Alegret, and E. Molina (2002), The Cretaceous/Palaeogene (K/P) boundary at Ain
625 Settara, Tunisia: restructuring of benthic foraminiferal assemblages, *Terra Nova*, 14(2), 101-107.
- 626 Quillevère, F., R. D. Norris, D. Kroon, and P. A. Wilson (2008), Transient ocean warming and
627 shifts in carbon reservoirs during the early Danian, *Earth and Planetary Science Letters*, 265(3-
628 4), 600-615.
- 629 Reitz, A., K. Pfeifer, G. J. de Lange, and J. Klump (2004), Biogenic barium and the detrital
630 Ba/Al ratio: a comparison of their direct and indirect determination, *Mar. Geol.*, 204(3-4), 289-
631 300.
- 632 Rocchia, R., D. Boclet, P. Bonte, L. Froget, B. Galbrun, C. Jehanno, and E. Robin (1992),
633 Iridium and other element distributions, mineralogy, and magnetostratigraphy near the
634 Cretaceous/Tertiary Boundary in Hole 761C, in *Proc. ODP, Sci. Results, 122*, edited by U. von
635 Rad, B. U. Haq and e. al., pp. 753-762, Ocean Drilling Program, College Station, TX.
- 636 Ryan, W. B. F., and e. al. (1979), Site 398, in *Init. Repts. DSDP, 47 part 2*, edited by J. Sibuet, -
637 C., W. B. F. Ryan and e. al., U.S. Govt. Printing Office, Washington.

- 638 Schulte, P., et al. (2010), The Chicxulub Asteroid Impact and Mass Extinction at the Cretaceous-
639 Paleogene Boundary, *Science*, 327(5970), 1214-1218.
- 640 Sepulveda, J., J. E. Wendler, R. E. Summons, and K. U. Hinrichs (2009), Rapid resurgence of
641 marine productivity after the Cretaceous-Paleogene mass extinction, *Science*, 326(5949), 129-
642 132.
- 643 Stilwell, J. D. (2003), Patterns of biodiversity and faunal rebound following the K-T boundary
644 extinction event in Austral Palaeocene molluscan faunas, *Palaeogeography Palaeoclimatology*
645 *Palaeoecology*, 195(3-4), 319-356.
- 646 Stott, L. D., and J. P. Kennett (1989), New constraints on early Tertiary paleoproductivity from
647 carbon isotopes in foraminifera, *Nature*, 342(6249), 526-529.
- 648 Stott, L. D., and J. P. Kennett (1990), The paleoceanographic and paleoclimatic signature of the
649 Cretaceous/Paleogene boundary in the Antarctic: stable isotopic results from ODP Leg 113, in
650 *Proc. ODP, Sci. Repts.*, 113, edited by P. F. Barker, J. P. Kennett and e. al., pp. 829-848, Ocean
651 Drilling Program, College Station, TX.
- 652 Thomas, E. (1990), Late Cretaceous through Neogene deep-sea benthic foraminifers (Maud Rise,
653 Weddell Sea, Antarctica), in *Proc. ODP, Sci. Repts.*, 113, edited by P. F. Barker, J. P. Kennett
654 and e. al., pp. 571-594, Ocean Drilling Program, College Station, TX.
- 655 Thomas, E. (2007), Cenozoic mass extinctions in the deep sea: what perturbs the largest habitat
656 on Earth?, in *Large ecosystem perturbations: causes and consequences: Geological Society of*
657 *America Special Paper 424*, edited by S. Monechi, R. Coccioni and M. R. Rampino, pp. 1–23.
- 658 Thomas, E., J. C. Zachos, and T. J. Bralower (2000), Deep-Sea Environments on a Warm Earth:
659 latest Paleocene - early Eocene, in *Warm Climates in Earth History*, edited by B. Huber, K.
660 MacLeod and S. Wing, pp. 132-160 Cambridge University Press.
- 661 Thompson, E. I., and B. Schmitz (1997), Barium and the late Paleocene delta C-13 maximum:
662 Evidence of increased marine surface productivity, *Paleoceanography*, 12(2), 239-254.
- 663 Wappler, T., E. D. Currano, P. Wilf, J. Rust, and C. C. Labandeira (2009), No post-Cretaceous
664 ecosystem depression in European forests? Rich insect-feeding damage on diverse middle
665 Palaeocene plants, Menat, France, *Proceedings of the Royal Society B-Biological Sciences*,
666 276(1677), 4271-4277.
- 667 Westerhold, T., U. Rohl, I. Raffi, E. Fornaciari, S. Monechi, V. Reale, J. Bowles, and H. F.
668 Evans (2008), Astronomical calibration of the Paleocene time, *Palaeogeography*
669 *Palaeoclimatology Palaeoecology*, 257(4), 377-403.
- 670 Widmark, J. G. V., and B. Malmgren (1992), Benthic foraminiferal changes across the
671 Cretaceous-Tertiary boundary in the deep sea - DSDP Site 525, Site 527, and Site 465, *J.*
672 *Foraminifer. Res.*, 22(2), 81-113.

- 673 Wilf, P., and K. R. Johnson (2004), Land plant extinction at the end of the Cretaceous: a
674 quantitative analysis of the North Dakota megafloral record, *Paleobiology*, 30(3), 347-368.
- 675 Zachos, J. C., and M. A. Arthur (1986), Paleoceanography of the Cretaceous/Tertiary Boundary
676 event: inferences from stable isotopic and other data, *Paleoceanography*, 1(1), 5-26.
- 677 Zachos, J. C., M. A. Arthur, and W. E. Dean (1989), Geochemical evidence for suppression of
678 pelagic marine productivity at the Cretaceous/Tertiary boundary, *Nature*, 337(6202), 61-64.
679
680
- 681

681 **FIGURE CAPTIONS**

682

683 **Figure 1. Map of change in export production across the K-Pg boundary as inferred from**
684 **multiple, independent proxies.** Paleoreconstruction of continental configuration 65 Mya
685 generated using ODSN plate reconstruction
686 (www.odsn.de/odsn/services/paleomap/paleomap.html).

687

688 **Figure 2. Barium proxies of export production in the latest Maastrichtian to early Danian**
689 **by relative age.** Ba/Ti and Ba/Fe ratios of total counts from XRF core scanning in dotted grey
690 and solid black respectively at (A) the Vigo Seamount (DSDP Hole 398D), North Atlantic, (B)
691 São Paulo (DSDP Site 356), South Atlantic, (C) Maud Rise (ODP Hole 690C), Antarctica, and
692 (F) Shatsky Rise (ODP Site 1209), North Pacific. Ba/Al, Ba/Fe, and Ba_{excess} in solid grey, solid
693 black and dotted black respectively and calculated from existing records of Ba (ppm), Al (ppm)
694 and Fe (ppm) for (D) Wombat Plateau (ODP Hole 761C), Indian Ocean [*Rocchia et al.*, 1992],
695 and (E) Shatsky Rise (DSDP Hole 577B) [*Michel et al.*, 1985]. The K-Pg boundary is placed at 0
696 million years in relative age.

697

698 **Figure 3. Full records of barium proxies of export production in the latest Maastrichtian to**
699 **early Danian by relative depth.** Ba/Ti and Ba/Fe ratios of total counts from XRF core scanning
700 in dotted grey and solid black respectively at (A) the Vigo Seamount, North Atlantic, (B) São
701 Paulo, South Atlantic, (C) Maud Rise, Antarctica, and (F) Shatsky Rise (ODP Site 1209), North
702 Pacific. Ba/Al, Ba/Fe, and Ba_{excess} in solid grey, solid black and dotted black respectively and
703 calculated from existing records of Ba (ppm), Al (ppm) and Fe (ppm) for (D) Wombat Plateau,

704 Indian Ocean [Rocchia *et al.*, 1992], and (E) Shatsky Rise 577B [Michel *et al.*, 1985]. The K-Pg
705 boundary is placed at 0 m relative depth. First (L) and last (T) occurrence of nannofossils (N)
706 and foraminifera (F) and magnetostratigraphy (M) indicate relative age in panels A-D. In panel
707 E, relative ages were obtained by tying the XFR Fe record of DSDP Hole 577B to ODP Site
708 1211 and Westerhold *et al.*'s [2008] age model (see Supplemental Table 5 for tie points). In
709 panel F, relative ages were obtained from a high-resolution study of cyclostratigraphy (C),
710 although age model uncertainties characterize the period indicated by the thick dashed line.

711

712 **Figure 4. Barium proxies of export production in the latest Maastrichtian to early Danian**
713 **at DSDP Site 577B, Shatsky Rise, North Pacific.** Ba/Ti ratios of total counts from XRF core
714 scanning in dotted grey against Ba/Al and Ba_{excess} measured with neutron-activation analysis
715 [Michel *et al.*, 1985] in solid grey and dotted black respectively. The K-Pg boundary is placed at
716 0 million years in relative age.

Figure 1.

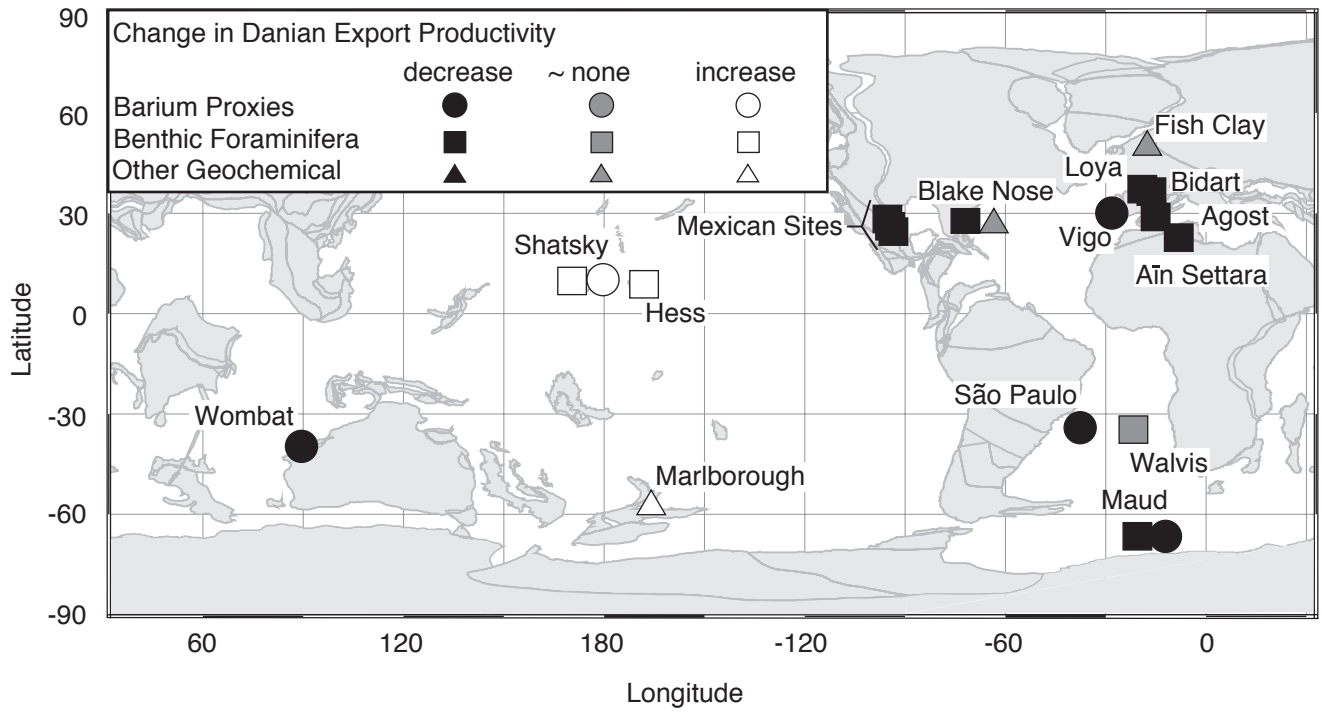


Figure 2.

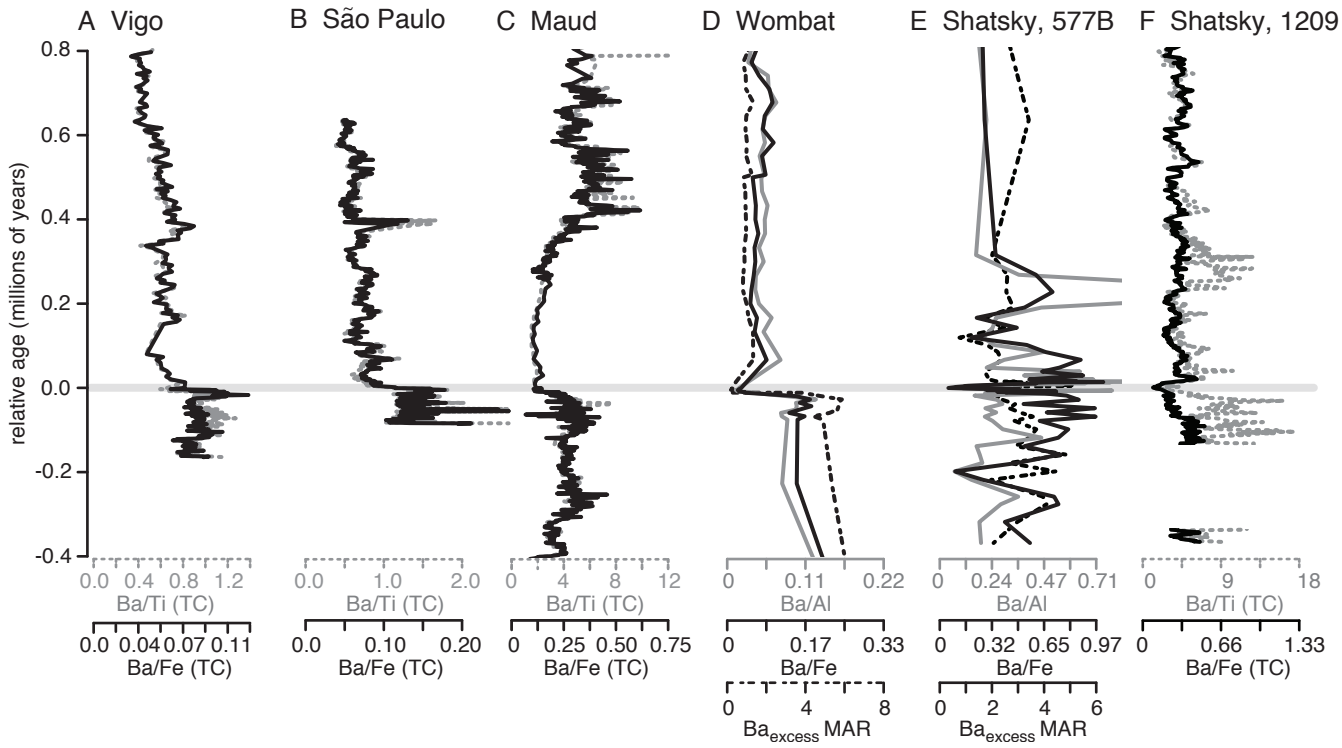


Figure 3.

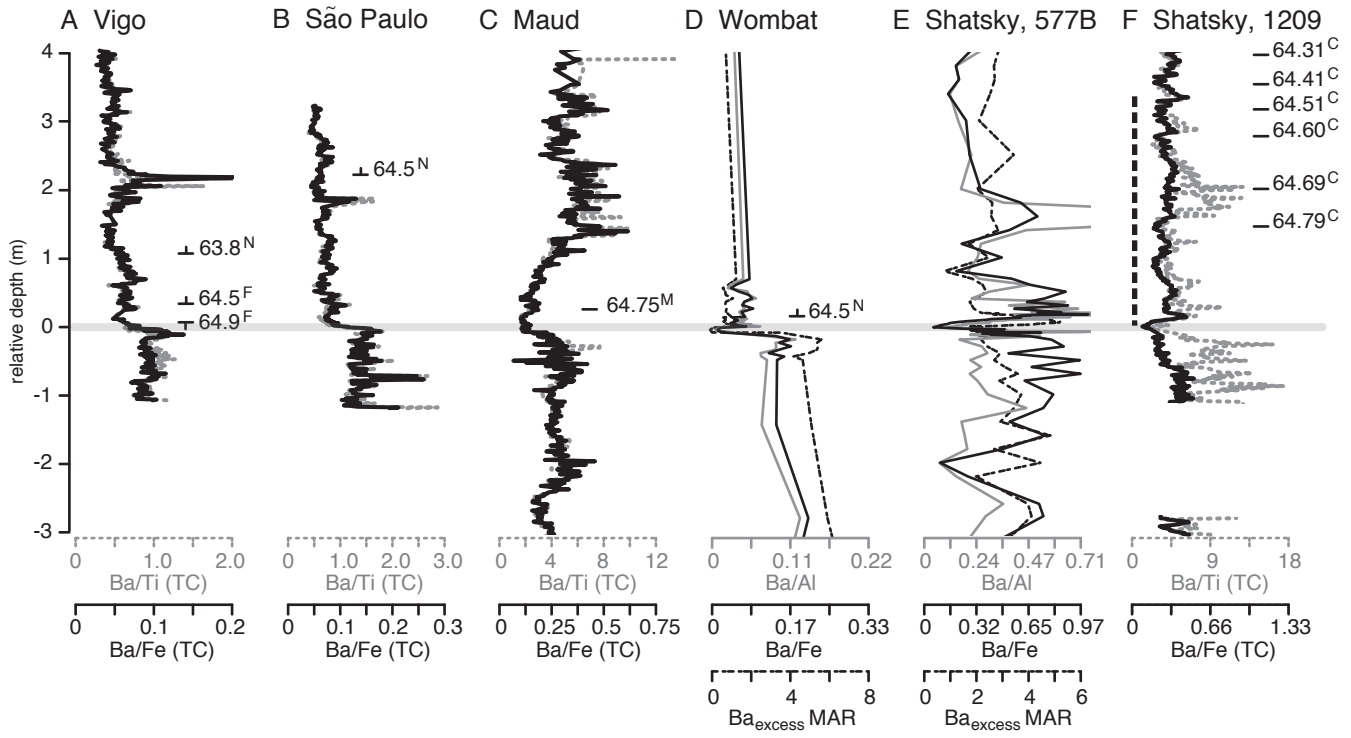


Figure 4.

